Acta Cryst E
CRYSTALLOGRAPHIC COMMUNICATIONS
ISSN 2056-9890

Synthesis, structural characterization, Hirshfeld surface analysis and QTAIM analysis of 3-(4-cyanothiophen-3-yl)-[1,2,4]selenadiazolo-[4,5-*a*]pyridin-4-ium chloride

Alexander A. Sapronov,[a] Evgeny A. Dukhnovsky,[a] Alexey S. Kubasov,[b] Alexander S. Novikov,[c] Maria M. Grishina,[a] Ekaterina V. Dobrokhotova,[a] Milena R. Komarovskikh,[a] Namiq Q. Shikhaliyev,[d] Mehmet Akkurt,[e] Ajaya Bhattarai[f]* and Alexander G. Tskhovrebov[g]

[a]Peoples' Friendship University of Russia, 6 Miklukho-Maklaya Street, Moscow, 117198, Russia, [b]Kurnakov Institute of General and Inorganic Chemistry, Russian Academy of Sciences, Leninsky Prosp. 31, 119071 Moscow, Russia, [c]Institute of Chemistry, Saint Petersburg State University, Universitetskaya Nab. 7/9, 199034 Saint Petersburg, Russia, [d]Department of Chemical Engineering, Baku Engineering University, Hasan Aliyev Street 120, Baku AZ0101, Azerbaijan, [e]Department of Physics, Faculty of Sciences, Erciyes University, 38039 Kayseri, Türkiye, [f]Department of Chemistry, M.M.A.M.C (Tribhuvan University) Biratnagar, Nepal, and [g]Research Institute of Chemistry, Peoples' Friendship University of Russia, Miklukho-Maklaya St., 6, Moscow 117198, Russian Federation. *Correspondence e-mail: ajaya.bhattarai@mmamc.tu.edu.np

Received 31 January 2025
Accepted 8 February 2025

Edited by B. Therrien, University of Neuchâtel, Switzerland

Keywords: crystal structure; chalcogen-hydrogen bonding; 1,2,4-selenodiazole; Hirshfeld surface analysis.

CCDC reference: 2300276

Supporting information: this article has supporting information at journals.iucr.org/e

The title compound, $C_{11}H_6N_3SSe^+\cdot Cl^-$, produced by the reaction between 3,4-dicyanothiophene and 2-pyridylselenyl chloride was isolated as a salt that crystallizes in the triclinic space group $P\overline{1}$. Notable features include strong chalcogen interactions (Se···Cl and Se···S), as revealed through Hirshfeld surface analysis, which also highlights significant contributions from N···H/H···N, C···H/H···C and H···H contacts in the crystal packing. Supramolecular interactions were further analysed using density functional theory (DFT) and quantum theory of atoms in molecules (QTAIM) at the ωB97XD/6–311++G** level of theory.

1. Chemical context

Recently, we discovered that 2-pyridylselenyl reagents undergo cyclization with unactivated nitriles under mild conditions, enabling the synthesis of previously unknown 1,2,4-selenadiazoles (Khrustalev *et al.*, 2021). The presence of two σ-holes on the selenium atom imparts a unique property to 1,2,4-selenadiazoles, allowing them to form supramolecular dimers *via* four-centre Se_2N_2 chalcogen bonds (Grudova *et al.*, 2022). Additionally, we explored their cycloaddition reactions with various nucleophilic molecules, demonstrating the versatility of 2-pyridylselenenyl reagents (Artemjev *et al.*, 2022, 2024; Sapronov *et al.*, 2022, 2024). In this report, we describe the structure of 3-(4-cyanothiophen-3-yl)-[1,2,4]-selenadiazolo[4,5-*a*]pyridin-4-ium chloride, which was obtained from the reaction between 3,4-dicyanothiophene and 2-pyridylselenenyl.

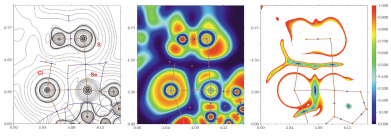

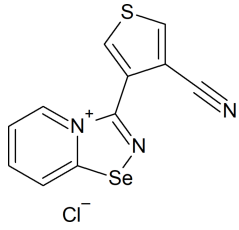

OPEN ACCESS
Published under a CC BY 4.0 licence

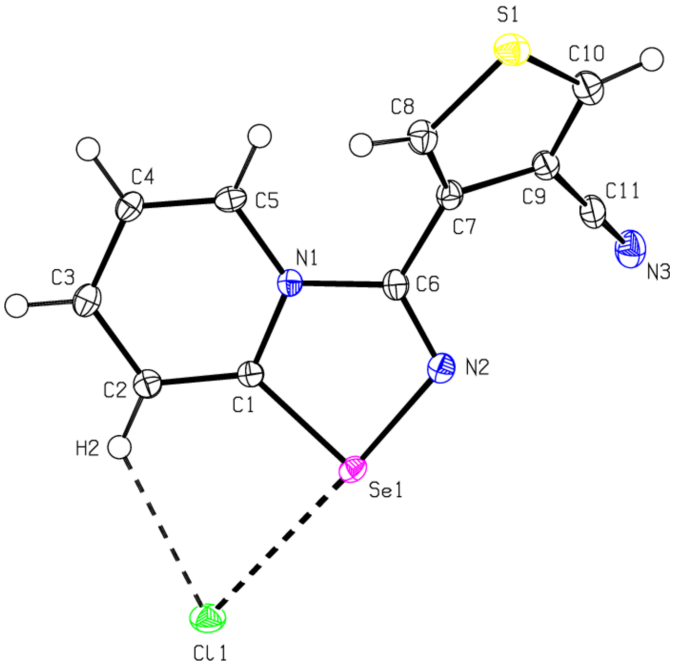

Figure 1
Molecular structure of 3-(4-cyanothiophen-3-yl)-[1,2,4]selenadiazolo[4,5-*a*]pyridin-4-ium chloride. Displacement ellipsoids are drawn at the 50% probability level.

2. Structural commentary

As shown in Fig. 1, the nine-membered ring system (Se1/N1/N2/C1–C6) of the cation is essentially planar [the maximum deviation is 0.034 (2) Å for C6] and makes an angle of 47.40 (9)° with the least-squares plane of the thiophene ring (S1/C7–C10). The intramolecular interaction between the Cl^- anion and the Se1 and (C2)H2 atoms of the cation forms an *S*(5) ring motif and thus the title molecule has a stable conformation. The Se1—C1 and Se1—N2 bond lengths are 1.865 (2) and 1.8511 (19) Å, respectively. The lengths of the single C6—N1 bond and the double C6—N2 bond are 1.426 (3) and 1.283 (3) Å, respectively. The bond length and angle values are comparable to those of similar compounds (see *Database survey* section).

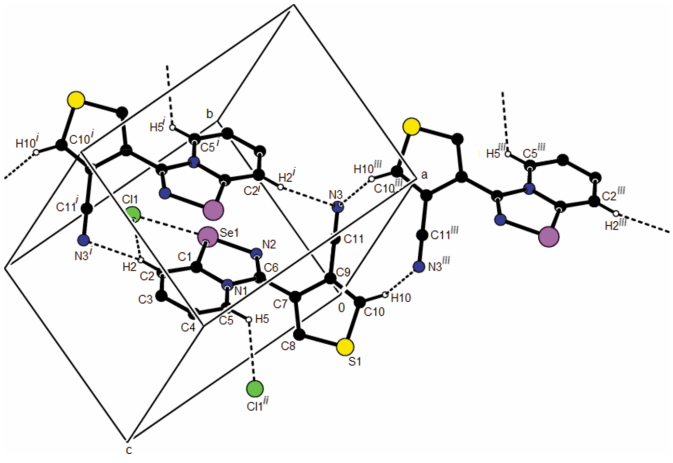

Figure 2
A partial packing diagram showing the C—H···N and C—H···Cl hydrogen bonds (dashed lines). H atoms not involved in these interactions have been omitted for clarity. Symmetry codes: (i) $-x+1, -y+1, -z+1$; (ii) $x, y-1, z$; (iii) $-x+1, -y, -z$.

Table 1
Hydrogen-bond geometry (Å, °).

D—H···A	D—H	H···A	D···A	D—H···A
C2—H2···Cl1	0.95	2.58	3.270 (3)	129
C2—H2···N3^{i}	0.95	2.62	3.285 (3)	127
C5—H5···Cl1^{ii}	0.95	2.66	3.316 (3)	127
C10—H10···N3^{iii}	0.95	2.52	3.154 (4)	124

Symmetry codes: (i) $-x+1, -y+1, -z+1$; (ii) $x, y-1, z$; (iii) $-x+1, -y, -z$.

3. Supramolecular features

In the crystal, pairs of cations are linked by C10—H10···N3 hydrogen bonds, thus forming a dimeric $R_2^2(10)$ ring motif (Table 1; Fig. 2; Bernstein *et al.*, 1995). These dimers are connected by pairs of C2—H2···N3 hydrogen bonds, forming inversion dimers with $R_2^2(18)$ ring motifs, which lead to the formation of ribbons propagating along the *c*-axis direction (Table 1). There are π–π stacking interactions between the rings of the bicyclic ring systems of two adjacent cations [Fig. 3; $Cg1\cdots Cg3^{i}$ = 3.964 (2) Å, slippage = 1.955 Å;

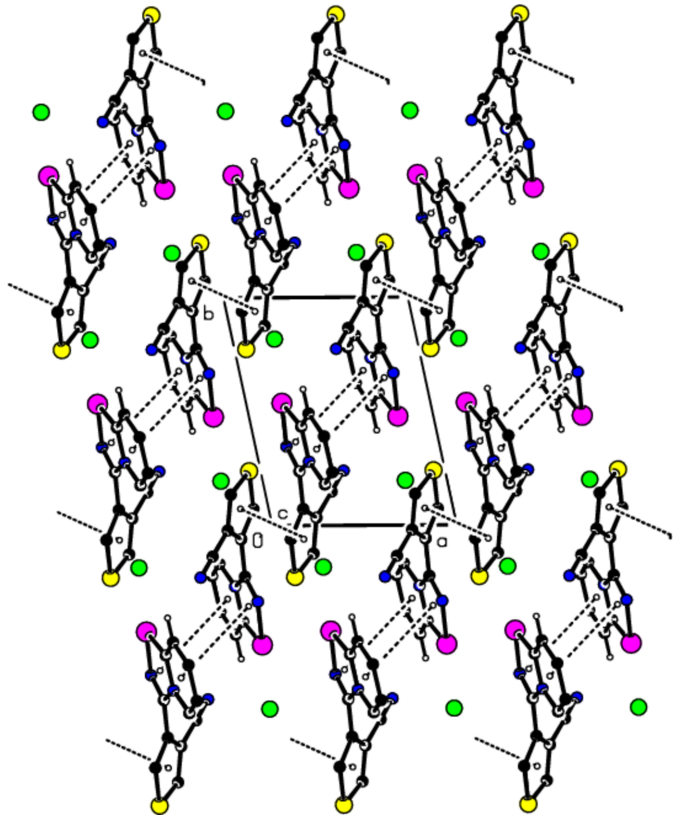

Figure 3
Crystal packing showing the π-π- stacking interactions between adjacent cations (dashed lines).

Table 2
Interatomic contacts (Å).

Contact	Distance	Symmetry operation
H2···Cl1	2.58	x, y, z
Se1···S1	3.66	$x, 1 + y, z$
C2···Se1	3.56	$-x, 1 - y, 1 - z$
H2···N3	2.62	$1 - x, 1 - y, 1 - z$
S1···Se1	3.66	$x, -1 + y, z$
C10···C9	3.41	$-x, -y, -z$
N1···Cl1	3.39	$-x, 1 - y, 1 - z$
N3···H3	2.66	$x, y, -1 + z$
H10···N3	2.52	$1 - x, -y, -z$
H5···Cl1	2.66	$x, -1 + y, z$
H8···C4	3.03	$-x, -y, 1 - z$
H4···C10	2.97	$1 - x, -y, 1 - z$

$Cg3\cdots Cg1^{i}$ = 3.964 (2) Å, slippage = 1.851 Å; symmetry code: (i) $-x + 1, -y + 1, -z + 1$; $Cg1$ and $Cg3$ are the centroids of the Se1/N2/C6/N1/C1 and N1/C1–C5 rings, respectively], as well as between two thiophene groups (Fig. 3). The distance between the centroids ($Cg2$ and $Cg2^{iv}$) of the thiophene rings (S1/C7–C10) is 3.849 (2) Å [slippage = 1.831 Å; symmetry code: (iv) $-x, -y, -z$]. These π–π stacking interactions between thiophene rings form ribbons along the [110] direction. Overall, the crystal is consolidated by this three-dimensional network formed by π-π stacking interactions and intermolecular C—H···N interactions.

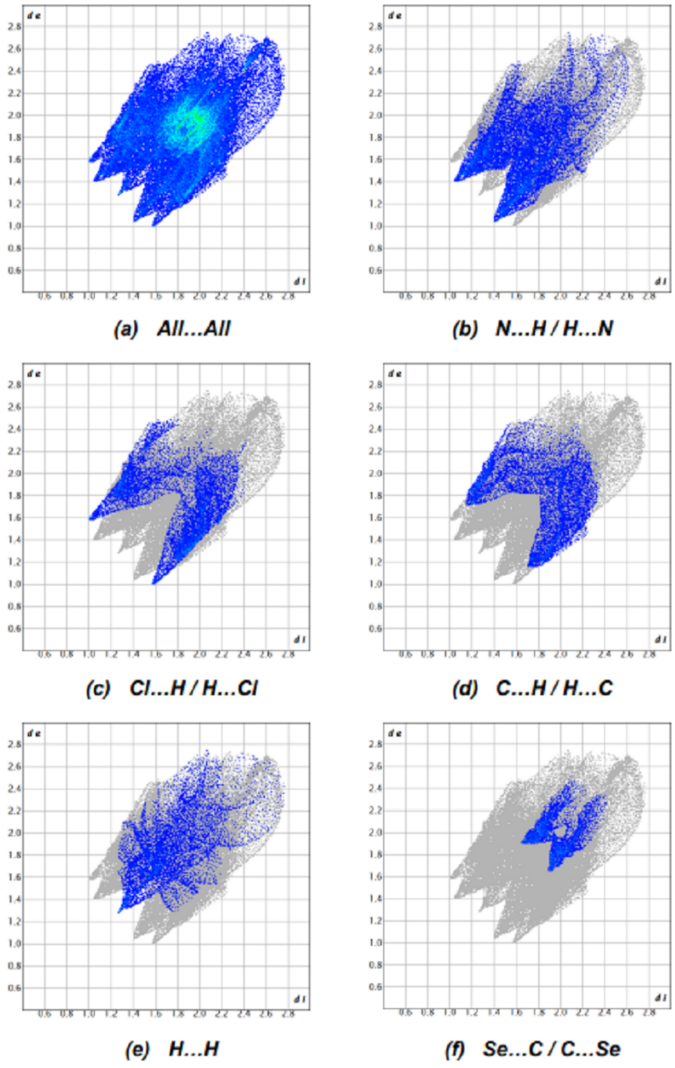

Figure 4
The two-dimensional fingerprint plots, showing (*a*) all interactions, and those delineated into (*b*) N···H/H···N, (*c*) Cl···H/H···Cl, (*d*) C···H/H···C, (*e*) H···H and (*f*) Se···C/C···Se interactions; d_e and d_i represent the distances from a point on the Hirshfeld surface to the nearest atoms outside (external) and inside (internal) the surface, respectively.

Table 3
Values of QTAIM parameters at the bond-critical points (3, −1), corresponding to chalcogen bonds Se···Cl and Se···S in the X-ray structure.

$\rho(\mathbf{r})$ = density of all electrons, $\nabla^2\rho(\mathbf{r})$ = Laplacian of electron density, λ_2 = eigenvalue, $[H_b]$ = energy density, $V(\mathbf{r})$ = potential energy density, $G(\mathbf{r})$ = Lagrangian kinetic energy, ELF (a.u.) = electron localization function and E_{int} = estimated strength for these interactions (kcal mol^{-1})

Contact[a]	Se···Cl, 2.843 Å, 78% vdW sum	Se···S, 3.656 Å, 99% vdW sum
$\rho(\mathbf{r})$	0.030	0.006
$\nabla^2\rho(\mathbf{r})$	0.067	0.020
λ_2	−0.030	−0.006
H_b	−0.001	0.001
$V(\mathbf{r})$	−0.019	−0.003
$G(\mathbf{r})$	0.018	0.004
ELF	0.178	0.024
E_{int}	6.0	0.9

Note: (*a*) The van der Waals (vdW) radii for S, Se, and Cl atoms are 1.80, 1.90, and 1.75 Å, respectively (Bondi, 1966).

4. Hirshfeld surface analysis

In order to quantify the intermolecular interactions in the crystal, *Crystal Explorer 17.5* (Spackman *et al.*, 2021) was used to generate Hirshfeld surfaces and two-dimensional fingerprint plots (Fig. 4). The most important interatomic contact is N···H/H···N as it makes the highest contribution to the crystal packing (22.2%, Fig. 4*b*). The other major contributors are the Cl···H/H···Cl (13.4%, Fig. 4*c*), C···H/H···C (12.4%, Fig. 4*d*) and H···H (11.3%, Fig. 4*e*) interactions. Other, smaller contributions (Table 2) are made by Se···C/C···Se (6.9%, Fig. 4*f*), Cl···C/C···Cl (5.3%), S···H/H···S (4.8%), S···N/N···S (4.4%), C···C (3.7%), Se···S/S···Se (3.6%), S···C/C···S (3.1%), Se···H/H···Se (2.4%), Cl···N/N···Cl (2.3%), C···N/N···C (2.2%), S···S (1.0%), Se···N/N···Se (0.9%) and Se···Cl/Cl···Se (0.1%) interactions.

5. QTAIM analysis

Inspection of the crystallographic data reveals the presence of Se···Cl and Se···S chalcogen bonds as being the most non-trivial non-covalent interactions. To better understand the nature and approximately quantify the strength of these intermolecular contacts, DFT calculations followed by topological analysis of the electron density distribution (QTAIM analysis) were carried out at the ωB97XD/6-311++G** level of theory. Results of the QTAIM analysis for chalcogen bonds Se···Cl and Se···S are summarized in Table 3; the contour line diagram of the Laplacian of electron density distribution $\nabla^2\rho(\mathbf{r})$, bond paths, and selected zero-flux surfaces, visualization of the electron localization function (ELF) and reduced

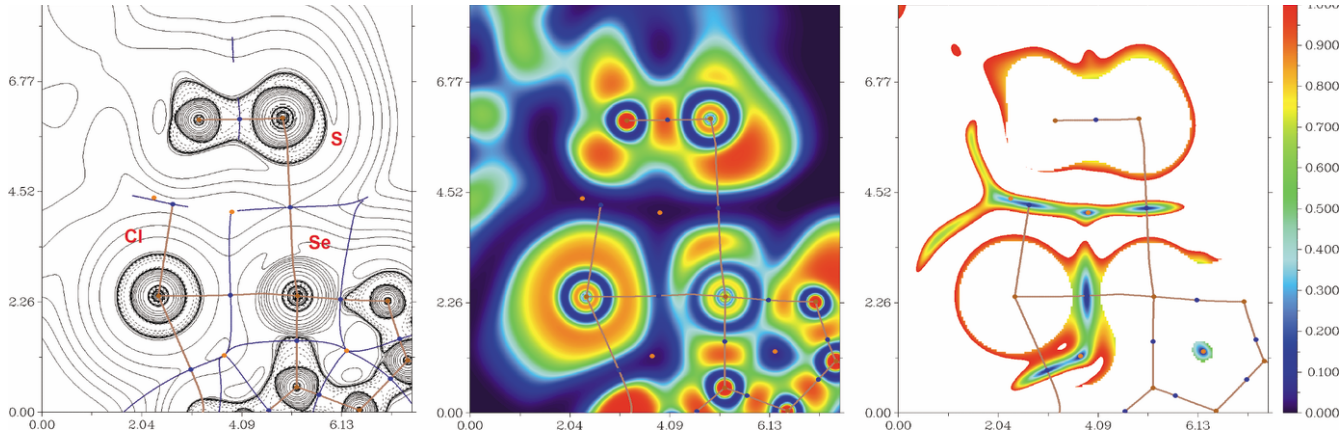

Figure 5
Contour line diagram of the Laplacian of electron density distribution $\nabla^2\rho(\mathbf{r})$, bond paths, and selected zero-flux surfaces (left panel), visualization of electron localization function (ELF, centre panel) and reduced density gradient (RDG, right panel) analyses for chalcogen bonds Se···Cl and Se···S. Bond critical points (3, −1) are shown in blue, nuclear critical points (3, −3) in pale brown and ring critical points (3, +1) in orange. Bond paths are shown as pale-brown lines, length are in Å, and the colour scale for the ELF and RDG maps is presented in a.u.

density gradient (RDG) analyses for these non-covalent contacts are shown in Fig. 5.

The QTAIM analysis of the model supramolecular associate demonstrates the presence of bond critical points (3, −1) for chalcogen bonds Se···Cl and Se···S (Table 3 and Fig. 5). The low magnitude of the electron density, the positive values of the Laplacian of electron density, very close to zero values of energy density, magnitudes of the electron localization function in these bond critical points (3, −1) and the estimated strengths for appropriate short contacts are typical for chalcogen bonds (Khrustalev *et al.*, 2021; Mikherdov *et al.*, 2016, 2018). The balance between the Lagrangian kinetic energy $G(\mathbf{r})$ and potential energy density $V(\mathbf{r})$ in bond critical points (3, −1) for chalcogen bonds Se···Cl and Se···S reveals that Se···S contacts are purely non-covalent, whereas Se···Cl contacts have small covalent contribution, (Espinosa *et al.*, 2002) and the sign of λ_2 allows these chalcogen bonds to be designated as bonding (attractive, $\lambda_2 < 0$) interactions (Johnson *et al.*, 2010; Contreras-García *et al.*, 2011).

6. Database survey

A search in the Cambridge Structural Database (CSD, Version 5.43, update of September 2022; Groom *et al.*, 2016) gave only 17 hits for 1,2,4-selenodiazolium salts. The most relevant salts are EHAPUC (Temesgen *et al.*, 2024), BEYHEW, BEYHIA, BEYHOG, BEYHUM, BEYJAU, BEYJEY, BEYJIC, BEYJOI and BEYJUO (Sapronov *et al.*, 2022). The molecules of EHAPUC are packed in layers parallel to the *ac* plane. Each row of 1,2,4-selenodiazolium salts in the layer is located antiparallel to the adjacent one. In addition to Se···Cl contacts, the anions form C—H···Cl contacts that link the cations and anions both within the layers and between them. BEYHEW, BEYHIA, BEYHOG, BEYHUM, BEYJAU, BEYJEY, BEYJIC, BEYJOI and BEYJUO promote the formation of self-assembled dimers with the recurrent Se_2N_2 supramolecular motif. The dimers are further consolidated by two symmetry-equivalent selenium–arene chalcogen-bond interactions.

7. Synthesis and crystallization

2-Pyridylselenyl chloride was synthesized by a published method (Artemjev *et al.*, 2023; Khrustalev *et al.*, 2021). A solution of $PhICl_2$ (26 mg, 96 µmol) in CH_2Cl_2 (2 mL) was added to a solution of 2,2′-dipyridyldiselenide (30 mg, 96 µmol) and thiophene-3,4-dicarbonitrile (13 mg, 96 µmol) in CH_2Cl_2 (2 mL), and the reaction mixture was left without stirring at room temperature for 12 h. After that, the solution was decanted to leave a yellow precipitate. The solid was washed with Et_2O (3 × 1 mL) and dried under vacuum. Yield: 40 mg (65%). ^{1}H NMR (700 MHz, D_2O) δ 9.43 (*d*, *J* = 6.8 Hz, 1H), 8.91 (*d*, *J* = 8.7 Hz, 1H), 8.67 (*d*, *J* = 3.0 Hz, 1H), 8.48–8.45 (*m*, 1H), 8.39 (*d*, *J* = 3.0 Hz, 1H), 8.01 (*dd*, *J* = 7.7, 6.5 Hz, 1H). ^{13}C NMR (176 MHz, D_2O) δ 168.4, 149.7, 141.0, 140.0, 136.8, 133.4, 127.5, 126.0, 123.3, 114.0, 110.6.

8. Refinement

Crystal data, data collection and structure refinement details are summarized in Table 4. The hydrogen atoms were placed in calculated positions and refined as riding models with fixed isotropic displacement parameters [U_{iso}(H) = 1.5U_{eq}(O), 1.5U_{eq}(C) for the CH_3-groups and 1.2U_{eq}(C) for the other groups]. The remaining positive and negative residual electron densities are both located near the selenium atom.

Acknowledgements

This work was performed under the support of the Russian Science Foundation (award No. 2273–10007). The author's contributions are as follows. Conceptualization, NQS, MA and

AB; synthesis, AAS, EAD, ASK and ASN; X-ray analysis, VNK and MA; writing (review and editing of the manuscript) MMG, MA and AB; funding acquisition, NQS, EVD and MRK; supervision, NQS and AGT.

References

Artemjev, A. A., Kubasov, A. S., Zaytsev, V. P., Borisov, A. V., Kritchenkov, A. S., Nenajdenko, V. G., Gomila, R. M., Frontera, A. & Tskhovrebov, A. G. (2023). *Cryst. Growth Des.* **23**, 2018–2023.

Artemjev, A. A., Novikov, A. P., Burkin, G. M., Sapronov, A. A., Kubasov, A. S., Nenajdenko, V. G., Khrustalev, V. N., Borisov, A. V., Kirichuk, A. A., Kritchenkov, A. S., Gomila, R. M., Frontera, A. & Tskhovrebov, A. G. (2022). *Int. J. Mol. Sci.* **23**, 6372.

Artemjev, A. A., Sapronov, A. A., Kubasov, A. S., Peregudov, A. S., Novikov, A. S., Egorov, A. R., Khrustalev, V. N., Borisov, A. V., Matsulevich, Z. V., Shikhaliyev, N. G., Nenajdenko, V. G., Gomila, R. M., Frontera, A., Kritchenkov, A. S. & Tskhovrebov, A. G. (2024). *Int. J. Mol. Sci.* **25**, 12798.

Bernstein, J., Davis, R. E., Shimoni, L. & Chang, N.-L. (1995). *Angew. Chem. Int. Ed. Engl.* **34**, 1555–1573.

Bondi, A. (1966). *J. Phys. Chem.* **70**, 3006–3007.

Bruker (2019). *SAINT*. Bruker Nano Inc. Madison, Wisconsin, USA.

Contreras-García, J., Johnson, E. R., Keinan, S., Chaudret, R., Piquemal, J.-P., Beratan, D. N. & Yang, W. (2011). *J. Chem. Theory Comput.* **7**, 625–632.

Espinosa, E., Alkorta, I., Elguero, J. & Molins, E. (2002). *J. Chem. Phys.* **117**, 5529–5542.

Farrugia, L. J. (2012). *J. Appl. Cryst.* **45**, 849–854.

Groom, C. R., Bruno, I. J., Lightfoot, M. P. & Ward, S. C. (2016). *Acta Cryst.* B**72**, 171–179.

Grudova, M. V., Khrustalev, V. N., Kubasov, A. S., Strashnov, P. V., Matsulevich, Z. V., Lukiyanova, J. M., Borisova, G. N., Kritchenkov, A. S., Grishina, M. M., Artemjev, A. A., Buslov, I. V., Osmanov, V. K., Nenajdenko, V. G., Trung, N. Q., Borisov, A. V. & Tskhovrebov, A. G. (2022). *Cryst. Growth Des.* **22**, 313–322.

Johnson, E. R., Keinan, S., Mori-Sánchez, P., Contreras-García, J., Cohen, A. J. & Yang, W. (2010). *J. Am. Chem. Soc.* **132**, 6498–6506.

Khrustalev, V. N., Grishina, M. M., Matsulevich, Z. V., Lukiyanova, J. M., Borisova, G. N., Osmanov, V. K., Novikov, A. S., Kirichuk, A. A., Borisov, A. V., Solari, E. & Tskhovrebov, A. G. (2021). *Dalton Trans.* **50**, 10689–10691.

Krause, L., Herbst-Irmer, R., Sheldrick, G. M. & Stalke, D. (2015). *J. Appl. Cryst.* **48**, 3–10.

Mikherdov, A. S., Kinzhalov, M. A., Novikov, A. S., Boyarskiy, V. P., Boyarskaya, I. A., Dar'in, D. V., Starova, G. L. & Kukushkin, V. Yu. (2016). *J. Am. Chem. Soc.* **138**, 14129–14137.

Mikherdov, A. S., Novikov, A. S., Kinzhalov, M. A., Zolotarev, A. A. & Boyarskiy, V. P. (2018). *Crystals*, **8**, 112.

Table 4
Experimental details.

Crystal data	
Chemical formula	$C_{11}H_6N_3SSe^+\cdot Cl^-$
M_r	326.66
Crystal system, space group	Triclinic, $P\overline{1}$
Temperature (K)	100
a, b, c (Å)	7.142 (3), 8.824 (4), 10.255 (5)
α, β, γ (°)	101.566 (13), 107.022 (14), 97.55 (1)
V (Å^3)	592.8 (5)
Z	2
Radiation type	Mo $K\alpha$
μ (mm^{-1})	3.55
Crystal size (mm)	0.60 × 0.40 × 0.10
Data collection	
Diffractometer	Bruker D8 Venture
Absorption correction	Multi-scan (*SADABS*; Krause *et al.*, 2015)
T_{min}, T_{max}	0.470, 0.746
No. of measured, independent and observed [$I > 2\sigma(I)$] reflections	7083, 3934, 3411
R_{int}	0.035
$(\sin \theta/\lambda)_{max}$ (Å^{-1})	0.755
Refinement	
$R[F^2 > 2\sigma(F^2)]$, $wR(F^2)$, S	0.034, 0.081, 1.05
No. of reflections	3934
No. of parameters	154
H-atom treatment	H-atom parameters constrained
$\Delta\rho_{max}$, $\Delta\rho_{min}$ (e Å^{-3})	1.22, −0.74

Computer programs: *SAINT* (Bruker, 2019), *SHELXT* (Sheldrick, 2015*a*), *SHELXL2018* (Sheldrick, 2015*b*), *ORTEP-3 for Windows* (Farrugia, 2012) and *PLATON* (Spek, 2020).

Sapronov, A. A., Artemjev, A. A., Burkin, G. M., Khrustalev, V. N., Kubasov, A. S., Nenajdenko, V. G., Gomila, R. M., Frontera, A., Kritchenkov, A. S. & Tskhovrebov, A. G. (2022). *Int. J. Mol. Sci.* **23**, 14973.

Sapronov, A. A., Khrustalev, V. N., Chusova, O. G., Kubasov, A. S., Kritchenkov, A. S., Nenajdenko, V. G., Gomila, R. M., Frontera, A. & Tskhovrebov, A. G. (2024). *Inorg. Chem.* **63**, 13924–13937.

Sheldrick, G. M. (2015*a*). *Acta Cryst.* A**71**, 3–8.

Sheldrick, G. M. (2015*b*). *Acta Cryst.* C**71**, 3–8.

Spackman, P. R., Turner, M. J., McKinnon, J. J., Wolff, S. K., Grimwood, D. J., Jayatilaka, D. & Spackman, M. A. (2021). *J. Appl. Cryst.* **54**, 1006–1011.

Spek, A. L. (2020). *Acta Cryst.* E**76**, 1–11.

Temesgen, A. W., Sapronov, A. A., Kubasov, A. S., Novikov, A. S., Le, T. A. & Tskhovrebov, A. G. (2024). *Acta Cryst.* E**80**, 247–251.

supporting information

Acta Cryst. (2025). E**81** [https://doi.org/10.1107/S205698902500115X]

Synthesis, structural characterization, Hirshfeld surface analysis and QTAIM analysis of 3-(4-cyanothiophen-3-yl)-[1,2,4]selenadiazolo[4,5-*a*]pyridin-4-ium chloride

Alexander A. Sapronov, Evgeny A. Dukhnovsky, Alexey S. Kubasov, Alexander S. Novikov, Maria M. Grishina, Ekaterina V. Dobrokhotova, Milena R. Komarovskikh, Namiq Q. Shikhaliyev, Mehmet Akkurt, Ajaya Bhattarai and Alexander G. Tskhovrebov

Computing details

3-(4-Cyanothiophen-3-yl)-[1,2,4]selenadiazolo[4,5-*a*]pyridin-4-ium chloride

Crystal data

$C_{11}H_6N_3SSe^+\cdot Cl^-$
M_r = 326.66
Triclinic, $P\overline{1}$
a = 7.142 (3) Å
b = 8.824 (4) Å
c = 10.255 (5) Å
α = 101.566 (13)°
β = 107.022 (14)°
γ = 97.55 (1)°
V = 592.8 (5) Å^3
Z = 2
F(000) = 320
D_x = 1.830 Mg m^{-3}
Mo $K\alpha$ radiation, λ = 0.71073 Å
Cell parameters from 5323 reflections
θ = 2.4–32.5°
μ = 3.55 mm^{-1}
T = 100 K
Block, colourless
0.60 × 0.40 × 0.10 mm

Data collection

Bruker D8 Venture diffractometer
Radiation source: sealed X-ray tube
Graphite monochromator
Detector resolution: 5.6 pixels mm^{-1}
ω scans
Absorption correction: multi-scan (SADABS; Krause *et al.*, 2015)
T_{min} = 0.470, T_{max} = 0.746
7083 measured reflections
3934 independent reflections
3411 reflections with $I > 2\sigma(I)$
R_{int} = 0.035
θ_{max} = 32.4°, θ_{min} = 2.2°
h = −10→8
k = −12→12
l = −15→14

Refinement

Refinement on F^2
Least-squares matrix: full
$R[F^2 > 2\sigma(F^2)]$ = 0.034
$wR(F^2)$ = 0.081
S = 1.05
3934 reflections
154 parameters
0 restraints
Hydrogen site location: inferred from neighbouring sites
H-atom parameters constrained
$w = 1/[\sigma^2(F_o^2) + (0.0221P)^2 + 0.1631P]$ where $P = (F_o^2 + 2F_c^2)/3$
$(\Delta/\sigma)_{max}$ = 0.001
$\Delta\rho_{max}$ = 1.22 e Å^{-3}
$\Delta\rho_{min}$ = −0.74 e Å^{-3}

Special details

Geometry. All esds (except the esd in the dihedral angle between two l.s. planes) are estimated using the full covariance matrix. The cell esds are taken into account individually in the estimation of esds in distances, angles and torsion angles; correlations between esds in cell parameters are only used when they are defined by crystal symmetry. An approximate (isotropic) treatment of cell esds is used for estimating esds involving l.s. planes.

Fractional atomic coordinates and isotropic or equivalent isotropic displacement parameters (Å²)

	x	*y*	*z*	U_{iso}*/U_{eq}
Se1	0.19350 (3)	0.53066 (2)	0.38485 (2)	0.01314 (6)
S1	0.06346 (8)	−0.22986 (6)	0.13180 (6)	0.02063 (12)
N1	0.2726 (2)	0.27311 (19)	0.46985 (18)	0.0114 (3)
N2	0.1683 (3)	0.3416 (2)	0.25768 (19)	0.0151 (3)
N3	0.4496 (3)	0.2362 (2)	0.0365 (2)	0.0213 (4)
C1	0.2707 (3)	0.4265 (2)	0.5271 (2)	0.0117 (3)
C2	0.3256 (3)	0.4828 (2)	0.6731 (2)	0.0143 (4)
H2	0.323858	0.589089	0.713832	0.017*
C3	0.3824 (3)	0.3817 (3)	0.7575 (2)	0.0163 (4)
H3	0.419393	0.418052	0.856995	0.020*
C4	0.3855 (3)	0.2246 (2)	0.6958 (2)	0.0148 (4)
H4	0.425057	0.154979	0.753641	0.018*
C5	0.3317 (3)	0.1726 (2)	0.5530 (2)	0.0144 (4)
H5	0.335128	0.067141	0.511177	0.017*
C6	0.2087 (3)	0.2315 (2)	0.3197 (2)	0.0139 (4)
C7	0.1862 (3)	0.0675 (2)	0.2395 (2)	0.0144 (4)
C8	0.0845 (3)	−0.0641 (3)	0.2593 (2)	0.0186 (4)
H8	0.032150	−0.063504	0.334549	0.022*
C9	0.2484 (3)	0.0300 (2)	0.1180 (2)	0.0148 (4)
C10	0.1904 (3)	−0.1269 (3)	0.0492 (2)	0.0191 (4)
H10	0.217413	−0.172478	−0.033747	0.023*
C11	0.3608 (3)	0.1445 (3)	0.0728 (2)	0.0176 (4)
Cl1	0.22732 (8)	0.81017 (6)	0.59166 (6)	0.02006 (11)

Atomic displacement parameters (Å²)

	U^{11}	U^{22}	U^{33}	U^{12}	U^{13}	U^{23}
Se1	0.01299 (10)	0.01398 (11)	0.01459 (10)	0.00329 (7)	0.00538 (8)	0.00667 (7)
S1	0.0196 (3)	0.0153 (2)	0.0223 (3)	0.0013 (2)	0.0030 (2)	0.0015 (2)
N1	0.0108 (7)	0.0118 (8)	0.0116 (8)	0.0006 (6)	0.0042 (6)	0.0031 (6)
N2	0.0143 (8)	0.0171 (8)	0.0139 (8)	0.0031 (6)	0.0044 (7)	0.0045 (7)
N3	0.0198 (9)	0.0275 (10)	0.0181 (9)	0.0049 (8)	0.0082 (8)	0.0057 (8)
C1	0.0108 (9)	0.0123 (9)	0.0132 (9)	0.0022 (7)	0.0051 (7)	0.0038 (7)
C2	0.0144 (9)	0.0138 (9)	0.0149 (9)	0.0016 (7)	0.0053 (8)	0.0038 (7)
C3	0.0152 (10)	0.0191 (10)	0.0149 (10)	0.0015 (8)	0.0047 (8)	0.0063 (8)
C4	0.0142 (9)	0.0156 (9)	0.0144 (9)	0.0012 (7)	0.0036 (8)	0.0063 (8)
C5	0.0135 (9)	0.0114 (9)	0.0188 (10)	0.0017 (7)	0.0052 (8)	0.0058 (7)
C6	0.0128 (9)	0.0159 (9)	0.0129 (9)	0.0011 (7)	0.0051 (7)	0.0032 (7)
C7	0.0134 (9)	0.0161 (9)	0.0122 (9)	0.0024 (7)	0.0027 (7)	0.0029 (7)

C8	0.0197 (10)	0.0177 (10)	0.0166 (10)	0.0000 (8)	0.0057 (8)	0.0030 (8)
C9	0.0123 (9)	0.0180 (10)	0.0131 (9)	0.0045 (7)	0.0031 (7)	0.0027 (7)
C10	0.0148 (10)	0.0239 (11)	0.0167 (10)	0.0056 (8)	0.0039 (8)	0.0013 (8)
C11	0.0171 (10)	0.0232 (11)	0.0122 (9)	0.0064 (8)	0.0048 (8)	0.0022 (8)
Cl1	0.0238 (3)	0.0131 (2)	0.0243 (3)	0.00350 (19)	0.0087 (2)	0.0060 (2)

Geometric parameters (Å, º)

Se1—N2	1.8511 (19)	C3—C4	1.410 (3)
Se1—C1	1.865 (2)	C3—H3	0.9500
S1—C10	1.705 (2)	C4—C5	1.362 (3)
S1—C8	1.712 (2)	C4—H4	0.9500
N1—C1	1.366 (3)	C5—H5	0.9500
N1—C5	1.372 (3)	C6—C7	1.477 (3)
N1—C6	1.426 (3)	C7—C8	1.370 (3)
N2—C6	1.283 (3)	C7—C9	1.434 (3)
N3—C11	1.148 (3)	C8—H8	0.9500
C1—C2	1.397 (3)	C9—C10	1.368 (3)
C2—C3	1.381 (3)	C9—C11	1.440 (3)
C2—H2	0.9500	C10—H10	0.9500
N2—Se1—C1	87.24 (9)	C4—C5—H5	120.1
C10—S1—C8	92.64 (11)	N1—C5—H5	120.1
C1—N1—C5	121.45 (18)	N2—C6—N1	117.21 (19)
C1—N1—C6	113.64 (17)	N2—C6—C7	121.7 (2)
C5—N1—C6	124.91 (18)	N1—C6—C7	121.10 (18)
C6—N2—Se1	111.81 (15)	C8—C7—C9	111.61 (19)
N1—C1—C2	119.91 (19)	C8—C7—C6	125.30 (19)
N1—C1—Se1	110.02 (15)	C9—C7—C6	122.64 (18)
C2—C1—Se1	130.06 (16)	C7—C8—S1	111.62 (17)
C3—C2—C1	119.0 (2)	C7—C8—H8	124.2
C3—C2—H2	120.5	S1—C8—H8	124.2
C1—C2—H2	120.5	C10—C9—C7	112.93 (19)
C2—C3—C4	119.9 (2)	C10—C9—C11	123.21 (19)
C2—C3—H3	120.0	C7—C9—C11	123.85 (19)
C4—C3—H3	120.0	C9—C10—S1	111.19 (17)
C5—C4—C3	119.9 (2)	C9—C10—H10	124.4
C5—C4—H4	120.0	S1—C10—H10	124.4
C3—C4—H4	120.0	N3—C11—C9	179.7 (3)
C4—C5—N1	119.78 (19)		
C1—Se1—N2—C6	1.08 (15)	C5—N1—C6—N2	−176.41 (18)
C5—N1—C1—C2	−1.5 (3)	C1—N1—C6—C7	−175.22 (17)
C6—N1—C1—C2	178.63 (17)	C5—N1—C6—C7	4.9 (3)
C5—N1—C1—Se1	177.54 (14)	N2—C6—C7—C8	−129.2 (2)
C6—N1—C1—Se1	−2.4 (2)	N1—C6—C7—C8	49.5 (3)
N2—Se1—C1—N1	0.80 (14)	N2—C6—C7—C9	42.5 (3)
N2—Se1—C1—C2	179.7 (2)	N1—C6—C7—C9	−138.8 (2)

N1—C1—C2—C3	0.5 (3)	C9—C7—C8—S1	−0.5 (2)
Se1—C1—C2—C3	−178.32 (15)	C6—C7—C8—S1	172.03 (17)
C1—C2—C3—C4	0.4 (3)	C10—S1—C8—C7	0.06 (18)
C2—C3—C4—C5	−0.2 (3)	C8—C7—C9—C10	0.7 (3)
C3—C4—C5—N1	−0.7 (3)	C6—C7—C9—C10	−171.97 (19)
C1—N1—C5—C4	1.6 (3)	C8—C7—C9—C11	−179.0 (2)
C6—N1—C5—C4	−178.50 (18)	C6—C7—C9—C11	8.3 (3)
Se1—N2—C6—N1	−2.7 (2)	C7—C9—C10—S1	−0.7 (2)
Se1—N2—C6—C7	175.96 (15)	C11—C9—C10—S1	179.05 (17)
C1—N1—C6—N2	3.5 (3)	C8—S1—C10—C9	0.37 (18)

Hydrogen-bond geometry (Å, º)

D—H···*A*	*D*—H	H···*A*	*D*···*A*	*D*—H···*A*
C2—H2···Cl1	0.95	2.58	3.270 (3)	129
C2—H2···N3^{i}	0.95	2.62	3.285 (3)	127
C5—H5···Cl1^{ii}	0.95	2.66	3.316 (3)	127
C10—H10···N3^{iii}	0.95	2.52	3.154 (4)	124

Symmetry codes: (i) −*x*+1, −*y*+1, −*z*+1; (ii) *x*, *y*−1, *z*; (iii) −*x*+1, −*y*, −*z*.